Available online at www.sciencedirect.com
SCIENCE DIRECT®
Journal of Computational Physics 192 (2003) 471–493
JOURNAL OF COMPUTATIONAL PHYSICS
www.elsevier.com/locate/jcp

A numerical method for the solution of thermo- and electro-static problems for a medium with isolated inclusions

S.K. Kanaun *, S. Babaii Kochekseraii

Instituto Tecnológico y de Estudios Superiores de Monterrey, Campus Estado de México, División de Ingeniería y Arquitectura, Apdo. Postal 6-3, Módulo de Servicio Postal, Atizapán 52926, Mexico

Received 15 May 2003; received in revised form 24 July 2003; accepted 24 July 2003

Abstract

Gaussian approximating functions are used for the solution of the volume integral equation of thermo- and electro-statics for a medium with isolated inhomogeneous inclusions. These functions essentially simplify the construction of the final matrix of the system of linear algebraic equations to which the problem is reduced after the discretization. The method is developed for the solution of 2D and 3D problems and the numerical results are compared with the exact solutions of the problems for spherically layered inclusions. The so-called Edge Gaussian approximating functions are proposed for the improvement of the numerical solution near the borders of the inclusions.
© 2003 Elsevier B.V. All rights reserved.

Keywords: Composite material; Thermo- and electro-static field; Gaussian approximating function; Collocation method; Layered inclusion

1. Introduction

A class of composites that consist of a homogeneous matrix and a set of isolated inclusions (matrix composites) is widely used in a variety of applications. Calculation of physical fields in such composites is an important problem of the theory of inhomogeneous media. When a medium with an inhomogeneous inclusion of complex geometry is subjected to an arbitrary external field, the physical fields in such a medium may only be numerically calculated. The finite element method is not useful in this case because the matrix (background medium) occupies a much larger region than the inclusions. It is shown to be more appropriate to reduce the problem to the solution of the volume integral equations for the fields inside inclusions [1] and then to use numerical means of solving these equations.

The conventional numerical solutions of the volume integral equations are based on the following procedure. The region of integration is divided into a finite number of subregions and unknown functions

* Corresponding author. Tel.: +52-5864-5665; fax: +52-5864-5651.
E-mail address: kanaoun@itesm.mx (S.K. Kanaun).

0021-9991/$ - see front matter © 2003 Elsevier B.V. All rights reserved.
doi:10.1016/j.jcp.2003.07.010

(i.e., the components of the fields inside the inclusion) are approximated by standard (typically polynomial or spline) functions in every subregion (see, e.g. [2]). After applying the method of moments or the collocation method, the problem is reduced to the solution of a finite system of linear algebraic equations for the coefficients of the approximation. The components of the matrix of this system are integrals over the subregions. For problems of thermo- and electro-statics, these integrals are singular, and the complexity of their calculations depends on the type of approximating functions utilized and the geometry of the subregions. If standard approximating functions are used, a great portion of the computer time is spent in calculating these integrals.

In this study, a class of Gaussian approximation functions is used for the numerical solution of the volume integral equations of thermo- and electro-statics of inhomogeneous media. The idea to use these functions for the solution of a wide class of integral equations of mathematical physics belongs to V. Maz'ya. The theory of approximation by Gaussian functions was developed in the works of Maz'ya [3,4] and Maz'ya and Shmidt [5], the multiresolution analysis based on Gaussian functions was proposed in Maz'ya and Shmidt [6]. These functions were used for the solution of the integral equations of static and dynamic elasticity and electromagnetic diffraction problems in [7–9].

The use of the Gaussian approximating functions for the numerical solution of the problems under consideration has the following main advantage. The action of the integral operators of the problems in hand on such functions may be presented in a simple analytical form. As a result, the time for the calculation of the matrix of the linear system obtained after the discretization of the problem, is essentially reduced in comparison with the methods where conventional approximating functions are used. One should note that the main drawback of using the Gaussian functions for approximation of fields inside a compact region is that everyone of such functions will have a non-compact support. As a result, the main error of this approximation appears in the close vicinity of the border of the region where the fields are calculated. To improve the approximation near the borders, the so-called Edge Gaussian functions are introduced in this work. They are equal to zero outside the region occupied by the inclusion. It is shown that the action of the integral operators of the thermo- and electro-static problems on the Edge Gaussian functions is a combination of a finite number of standard functions. The latter may be simply tabulated, kept in the computer memory, and used for the solution of a wide class of the problems under consideration.

The present article is structured as follows.

The volume integral equations of thermo- and electro-statics and the properties of their solutions are considered in Section 2. Section 3 deals with some classes of analytical solutions of these equations. The case of a medium with a spherically symmetric inclusion subjected to a constant external field is considered here. Section 4 discusses the main properties of the approximations using the Gaussian functions and the Edge Gaussian functions. Section 5 presents the solution of the volume integral equations of thermo- and electro-statics in 2D-case using the Gaussian approximating functions. It is shown there, that if the pure Gaussian functions are used for the approximation of the solution, the elements of the matrix of the discretized problem obtained by the collocation method will have simple analytical forms. However, if the 2D-Edge Gaussian functions are used for the approximation, the components of the matrix of the discretized problem turn out to be combinations of two standard one-dimensional integrals that depend on three non-dimensional parameters. For small values of the parameters these integrals are tabulated and kept in the computer memory. Asymptotic expressions of these integrals for large values of parameters have forms of simple elementary functions. Examples of the numerical solutions of 2D-problems for layered inclusions and for inclusions with continuous property varying along the radius are presented in the same section. The numerical solutions are compared with the exact solutions of these problems.

In Section 6, the method is extended to the 3D-case. The action of the integral operator of the 3D-problems on the Gaussian and Edge Gaussian functions are obtained here. Similar to the 2D-case, the elements of the matrix of the discretized problem have simple analytical forms if the Gaussian functions are used for approximation. For the Edge Gaussian functions, such elements are combinations on some

standard integrals that depend on non-dimensional parameters. These integrals may be tabulated for small values of these parameters and will have simple asymptotic expressions for their large values. The numerical solutions of 3D-problems for spherically layered inhomogeneous inclusions are obtained and compared with the exact solutions of these problems in this section.

The final conclusions and the discussion of the area of application of the method are presented in Section 7.

The proposed method of the solution of the electro- and thermo-static problems for spherically layered inclusions is described in Appendix A.

2. The volume integral equations of thermo- and electro-statics for a homogeneous medium with an isolated inclusion

Let us consider an infinite homogeneous medium with the tensor of dielectric permittivity $\mathbf{C}_0$ containing an inhomogeneous inclusion with the dielectric permittivity $\mathbf{C}(x)$. The inclusion occupies region V with the characteristic function $V(x)$: $V(x) = 1$ if $x \in V$, $V(x) = 0$ if $x \notin V$. Here, x is a point of the medium with the Cartesian coordinates (x_1, x_2, x_3). If an external electric field $\mathbf{E}_0(x)$ is applied to the medium, the electric field $\mathbf{E}(x)$ in the medium including the inclusion, satisfies the following integral equation [1]:

$$E_i(x) + \int_V K_{ij}(x - x')C_{1jk}(x')E_k(x')\,\mathrm{d}x' = E_{0i}(x), \tag{2.1}$$

where $\mathbf{C}_1(x) = \mathbf{C}(x) - \mathbf{C}_0$,

$$K_{ij}(x) = -\partial_i\partial_j G(x), \quad \partial_i = \frac{\partial}{\partial x_i}. \tag{2.2}$$

Here $G(x)$ is the Green function of the homogeneous medium with the dielectric permittivity $\mathbf{C}_0$. $G(x)$ is the diminishing at infinity solution of the following equation:

$$\partial_i C_{0ij}\partial_j G(x) = -\delta(x), \tag{2.3}$$

where $\delta(x)$ is Dirac's delta-function. Summation with respect to repeating indexes is implied here. The electric displacement field $\mathbf{Z}(x)$ in the medium is defined as $\mathbf{Z}(x) = [\mathbf{C}_0 + \mathbf{C}_1(x)V(x)] \cdot \mathbf{E}(x)$ and satisfies the equation similar to Eq. (2.1)

$$Z_i(x) + \int_V S_{ij}(x - x')B_{1jk}(x')Z_k(x')\,\mathrm{d}x' = Z_{0i}(x). \tag{2.4}$$

Here, $\mathbf{B}_1(x) = \mathbf{B}(x) - \mathbf{B}_0$, $\mathbf{B}(x) = \mathbf{C}^{-1}(x)$, $\mathbf{B}_0 = \mathbf{C}_0^{-1}$, $\mathbf{Z}_0(x) = \mathbf{C}_0 \cdot \mathbf{E}_0(x)$, and the dot represents the scalar product of vectors and tensors,

$$S_{ij}(x) = C_{0ij}\delta(x) - C_{0ik}K_{kl}(x)C_{0lj}. \tag{2.5}$$

Note that Eq. (2.4) is a consequence of Eq. (2.1) and vice versa.

In the case of thermo-static problems, vector $\mathbf{E}(x)$ has another physical meaning. It is the gradient of the temperature field $T(x)$ $(E_i(x) = -\partial_i T(x))$, $\mathbf{Z}(x) = \mathbf{C}(x) \cdot \mathbf{E}(x)$ is the heat flux, and $\mathbf{C}(x)$ is the tensor of the coefficients of thermo-conductivity. But the equations for these quantities will have the same forms (2.1) and (2.4).

The integral operators with the kernels $\mathbf{K}(x)$ and $\mathbf{S}(x)$ in Eqs. (2.1) and (2.4) are pseudo-differential operators with the following symbols (Fourier transforms of the functions $\mathbf{K}(x)$ and $\mathbf{S}(x)$)

$$\widetilde{K}_{ij}(k) = \frac{k_i k_j}{k_l C_{0lm} k_l}, \quad \widetilde{S}_{ij}(k) = C_{0ij} - C_{0il}\widetilde{K}_{lm}(k) C_{0mj}. \tag{2.6}$$

These symbols are homogeneous functions of the order zero with respect to the vector parameter k of the Fourier transform. The action of these operators on a smooth function $f(x)$ with a finite support is defined as follows (see [10,11]):

$$(\mathbf{K}f)(x) = \int \mathbf{K}(x-x')f(x')\,\mathrm{d}x' = \mathbf{a}f(x) + \text{v.p.}\int \mathbf{K}(x-x')f(x')\,\mathrm{d}x', \tag{2.7}$$

$$(\mathbf{S}f)(x) = \int \mathbf{S}(x-x')f(x')\,\mathrm{d}x' = \mathbf{s}f(x) + \text{v.p.}\int \mathbf{S}(x-x')f(x')\,\mathrm{d}x'. \tag{2.8}$$

Here v.p. $\int \ldots \mathrm{d}x$ is the Cauchy principal value of the integral. Constants $\mathbf{a}$ and $\mathbf{s}$ have the forms [11]

$$\mathbf{a} = \frac{1}{\mathrm{mes}(\Omega_1)}\int_{\Omega_1} \tilde{\mathbf{K}}(k)\,\mathrm{d}k, \quad \mathbf{s} = \frac{1}{\mathrm{mes}(\Omega_1)}\int_{\Omega_1} \tilde{\mathbf{S}}(k)\,\mathrm{d}k, \tag{2.9}$$

where Ω_1 is the surface of the unit sphere in k-space of the Fourier transforms, $\mathrm{mes}(\Omega_1)$ is the area of this sphere.

If $f(x)$ is a smooth function with a non-compact support that tends to zero faster than any negative power of $|x|$ (class S), the action of the operator $\mathbf{K}$ and $\mathbf{S}$ on such a function may be presented in the following forms:

$$(\mathbf{K}f)(x) = \int \mathbf{K}(x-x')f(x')\,\mathrm{d}x' = \frac{1}{(2\pi)^d}\int \widetilde{\mathbf{K}}(k)\widetilde{f}(k)\exp(-\mathrm{i}k\cdot x)\,\mathrm{d}k, \tag{2.10}$$

$$(\mathbf{S}f)(x) = \int \mathbf{S}(x-x')f(x')\,\mathrm{d}x' = \frac{1}{(2\pi)^d}\int \widetilde{\mathbf{S}}(k)\widetilde{f}(k)\exp(-\mathrm{i}k\cdot x)\,\mathrm{d}k, \tag{2.11}$$

where d is the space dimension. Importantly, the right-hand sides of these equations exist as ordinary integrals.

It should be noted that Eqs. (2.1) and (2.4) are in fact the equations for the fields $\mathbf{E}(x)$ and $\mathbf{Z}(x)$ inside the region V occupied by the inclusion. The fields in the matrix medium may be reconstructed from Eqs. (2.1) and (2.4), if the fields inside the region V are known. Mikhlin [10] discussed in detail the conditions for the existence and uniqueness of the solutions of Eqs. (2.1) and (2.4). In short, the unique solutions of these equations exist if the determinants of the main homogeneous part of the symbols of the operators in the left-hand sides of these equations are not degenerated inside V. The latter is true, if $\mathbf{C}(x) \neq 0, \infty$ inside V. If $\mathbf{C}(x) = 0$ ($\mathbf{C}_1 = -\mathbf{C}_0$), the homogeneous equation (2.1) has a class of non-trivial solutions. Similarly, if $\mathbf{C}(x) \to \infty$ (i.e., $B_1 = -B_0$), the homogeneous equation (2.4) will have non-trivial solutions. As a result, the numerical solutions of the Eqs. (2.1) and (2.4) for very small or very large $\mathbf{C}(x)$ turn to be ill-posed problems.

The solutions of Eqs. (2.1) and (2.4) should jump on the border Ω of region V. Similarly, $\mathbf{E}(x)$ should jump on the surfaces were the function $\mathbf{C}(x)$ has discontinuities inside V. The jump of the function $\mathbf{E}(x)$ on Ω satisfies the following equation [11]:

$$\mathbf{E}^+(x) - \mathbf{E}^-(x) = \widetilde{\mathbf{K}}(\mathbf{n})\cdot\mathbf{C}_1(x)\cdot\mathbf{E}^-(x), \quad x \in \Omega, \tag{2.12}$$

where $\mathbf{E}^+(x)$ is the limit value of the field $\mathbf{E}(x)$ when $x \to \Omega$ and x is inside the region V, $\mathbf{E}^-(x)$ is the same limit of $\mathbf{E}(x)$ when $x \to \Omega$ from outside V, $\mathbf{n}$ is the external normal to Ω at point x. Function $\widetilde{\mathbf{K}}(\mathbf{n})$ is defined in Eq. (2.6).

3. Some analytical solutions of the integral equation (2.1)

In the case of a homogeneous ellipsoidal inclusion and a polynomial external field $\mathbf{E}_0(x)$, the solution of Eqs. (2.1) and (2.4) may be found in a closed analytical form. According to the polynomial conservativity theorem, a polynomial external field induces a polynomial polarization field inside any ellipsoidal inclusion. The method of constructing this field is discussed in [11].

Another class of analytical solutions may be constructed for a spherically symmetric inclusion subjected to a constant external field $\mathbf{E}_0$ [12]. Let us consider an isotropic medium with a spherical and isotropic inclusion centered at the origin of the Cartesian coordinate system. The dielectric properties of the inclusion depend only on the distance from the origin $C_{ij}(x) = c(|x|)\delta_{ij}$. Here, δ_{ij} is the Kronecker symbol. In the case of a constant external field $\mathbf{E}_0$, the electric field $\mathbf{E}(x)$ in the medium and inclusion takes the form (see Appendix A):

$$E_i(x) = E_{0i} + A_{ij}(r,n)E_{0j}, \quad r = |x|, \;\; n_j = \frac{x_j}{r}, \tag{3.1}$$

$$A_{ij}(r,n) = (\delta_{ij} + n_i n_j D)\alpha(r), \quad D = r\frac{\mathrm{d}}{\mathrm{d}r}. \tag{3.2}$$

The scalar function $\alpha(r)$ satisfies some ordinary differential equation of the second order (see Appendix A). In the case of a spherically layered inclusion, the function $c(r)$ is a stepwise constant function ($c(r) = c^{(i)}$ if $a^{(i-1)} < r < a^{(i)}$, $a^{(i-1)}$ and $a^{(i)}$ are internal and external radii of the ith layer), and the function $\alpha(r)$ inside the ith layer takes the form

$$\alpha(r) = Y_1^{(i)} + Y_2^{(i)} r^{-d}, \quad a^{(i-1)} < r < a^{(i)}, \;\; i = 1, 2, \ldots, \tag{3.3}$$

where $Y_1^{(i)}$, $Y_2^{(i)}$ are constants and d is the dimension of the space.

The algorithms for the construction of all the constants $Y_1^{(i)}$, $Y_2^{(i)}$ in 2D and 3D-cases are described in Appendix A. Using these algorithms, the solutions of the problem for the inclusion with a continuous property varying along the radius may be obtained by a stepwise constant approximation of the original function $c(r)$. The solution of the last problem converges to the solution of the continuously varying $c(r)$ problem, when the number of the layers tends to infinity in such a way that the maximal thickness of the layers tends to zero.

4. Gaussian approximating functions

The class of Gaussian approximating functions proposed in [3–6] will be used for the numerical solution of Eqs. (2.1) and (2.4). Let $u(x)$ be a scalar function in d-dimensional space $\mathbf{R}^d$. Assuming that $u(x)$ and its first derivative are bounded, $u(x)$ may be approximated by the following series:

$$u(x) \approx u_h(x) = \sum_{\mathbf{m}\in\mathbf{Z}^d} u_m \varphi(x - h\mathbf{m}), \quad \varphi(x) = \frac{1}{(\pi H)^{d/2}} \exp\left(-\frac{|x|^2}{Hh^2}\right). \tag{4.1}$$

Here $\mathbf{m} \in \mathbf{Z}^d$ is a d-dimensional vector with integer components, $h\mathbf{m}$ are the coordinates of the nodes of this approximation and h is the distance between the neighboring nodes, $u_m = u(h\mathbf{m})$ is the value of the function $u(x)$ at the node $x = h\mathbf{m}$, and H is a dimensionless parameter. It is demonstrated in [3–5] that the following estimation holds:

$$|u(x) - u_h(x)| \leqslant \beta h \|\nabla u\| + |u(x)|R(H), \quad R(H) = \mathrm{O}(\exp(-\pi^2 H)). \tag{4.2}$$

Here $\|\nabla u\|$ is the norm in the space of continuous functions, $\beta = \mathrm{O}(1)$. If h is sufficiently small, the error of the approximation (4.1) may be made negligible by the appropriate choice of the parameter H ($H = \mathrm{O}(1)$). The properties of this approximation were discussed in detail in [3–5].

Approximation (4.1) may be used for a wider class of functions, but the errors of the approximation may increase if the function does not satisfy the above-mentioned conditions. One of the causes of these errors is connected with non-compact supports of all the functions $\varphi(x - h\mathbf{m})$ in Eq. (4.1). This fact, strictly speaking, does not allow to approximate the functions with a compact support by the series in Eq. (4.1). Thus, the solutions of the integral equations (2.1) and (2.4) that should be constructed in a compact region V, will have an inevitable error if approximation (4.1) is used. Let consider the peculiarities of the approximation (4.1) in 1D-case for a function $v(x)$ that has a finite support

$$v(x) = \begin{cases} 1 + x^3, & |x| \leqslant 1; \\ 0, & |x| > 1. \end{cases} \tag{4.3}$$

The approximation (4.1) of this function is shown to be:

$$v_h(x) = \frac{1}{\sqrt{\pi H}} \sum_{i=1}^{N+1} v(x^{(i)}) \exp\left(- \frac{[x - x^{(i)}]^2}{Hh^2} \right) \tag{4.4}$$

and is presented in Figs. 1(a) and (b) for various values of the parameters H and h. The coordinates of the nodes are chosen at points $x^{(i)} = -1 + h(i-1)$, $i = 1, 2, \ldots, N+1$; $h = 2/N$, where $N + 1$ is the number of nodes inside the interval $[-1, 1]$. The bold solid lines in Figs. 1(a) and (b) are the function (4.3). The three thin lines in Fig. 1(a) correspond to $h = 0.2$ and different values of $H = 2$; 1; and 0.3. The three thin lines in Fig. 1(b) correspond to different values of $h = 0.1$; 0.2; and 0.05 and for $H = 0.7$. It is seen from this figure that the Gaussian approximation functions satisfactorily describe $v(x)$ in the middle region of the interval $[-1, 1]$ and near its left end $(x = -1)$, where $v(x)$ tends to zero. In the neighborhood of the right end of the interval, $(x = 1)$, where $v(x)$ has a finite jump, the error of the approximation (4.4) is maximal. This error decreases with decreasing values of h and H, but for $H < 0.5$, the error of the approximation in the middle region of the interval grows dramatically (see oscillation of $v_h(x)$ for $H = 0.3$ in Fig. 1(a)).

In order to improve the quality of the approximation (4.1) near the right end of the interval $[-1, 1]$ let us introduce the Edge Gaussian function defined by the equation

$$\widehat{\varphi}(x, b) = \begin{cases} \frac{1}{\sqrt{\pi H}} \exp\left(- \frac{x^2}{Hh^2} \right), & x \leqslant b; \\ 0, & x > b. \end{cases} \tag{4.5}$$

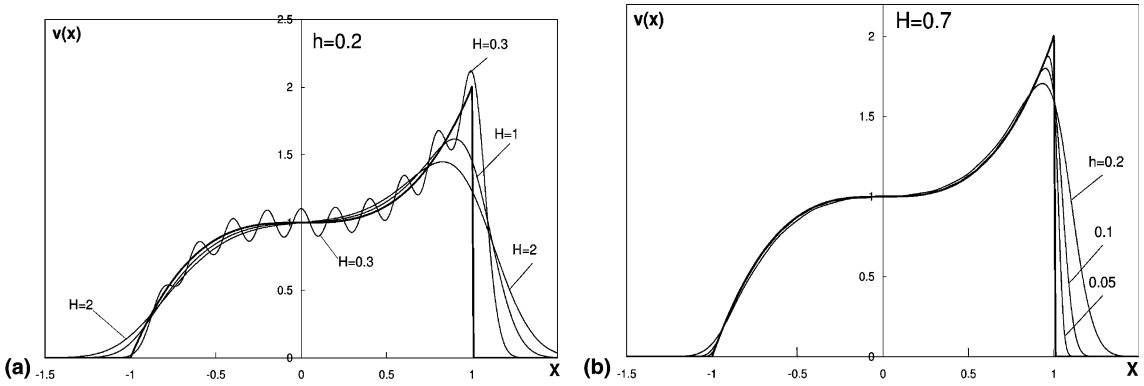

Fig. 1. Approximation of the function $v(x) = (1 + x^3)$, $|x| \leqslant 1$; $v(x) = 0$, $|x| > 1$ by the Gaussian functions.

Function

$$\widehat{v}_h(x) = \sum_{i=1}^{N+1} v(x^{(i)})\widehat{\varphi}\left[\mathrm{sign}(x)(x - x^{(i)}), b^{(i)}\right], \quad b^{(i)} = 1 - |x^{(i)}| \tag{4.6}$$

coincides with function $v_h(x)$ in Eq. (4.4) inside the interval $[-1, 1]$ and is equal to zero outside it. Here, $b^{(i)}$ is the shortest distance of the node $x^{(i)}$ from the ends of the interval $[-1, 1]$. Thus, the Edge Gaussian function (4.5) allows to cut the approximation (4.4) inside the region, where the original function is not equal to zero, and essentially improve the approximation of the considered function in the neighborhood of the right end of the interval. (The thin lines inside the interval $[-1, 1]$ in Fig. 1(b) correspond to $\widehat{v}_h(x)$, and $\widehat{v}_h(x) = 0$ if $|x| > 1$.)

In the 2D and 3D-cases, the Edge Gaussian functions may be introduced as follows:

$$\widehat{\varphi}(x, b) = \begin{cases} \frac{1}{(\pi H)^{d/2}} \exp\left(-\frac{|x|^2}{Hb^2}\right), & x_d \leqslant b; \\ 0, & x_d > b, \end{cases} \tag{4.7}$$

where $|x| = \sqrt{\sum_{k=1}^{d} x_k^2}$ and d is the dimension of the space. The proper use of the Edge Gaussian functions necessitates the introduction of a local Cartesian coordinate system at every node $x^{(i)}$. The axis x_d of this system should coincide with the direction of the shortest line connecting the ith node to the border Ω of the region V, where the approximating function is not equal to zero. $b^{(i)}$ is the length of this line. An arbitrary function $u(x)$ may be approximated by the Edge Gaussian functions in the form:

$$u(x) \approx \sum_{i=1}^{M} u(x^{(i)})\widehat{\varphi}\left((x - x^{(i)})_1, \ldots, (x - x^{(i)})_d, b^{(i)}\right), \tag{4.8}$$

where $(x - x^{(i)})_j$ $(j = 1, \ldots, d)$ are the coordinates of vector $x - x^{(i)}$ in the local basis of the ith node. The detailed formulations of these approximations in the 2D and 3D-cases are presented in Sections 5 and 6, below.

5. Numerical solution of Eq. (2.1) in the 2D-case

5.1. Gaussian approximating functions

Let an infinite isotropic 2D-medium with the dielectric permittivity c_0 contain an inclusion in the region V with the dielectric permittivity $c(x)$. The solution of the integral equation (2.1) inside this region could be found in the form similar to (4.1) as:

$$\begin{aligned} &\mathbf{E}(x) \approx \sum_{l=1}^{M} \mathbf{E}^{(l)}\varphi(x - x^{(l)}), \\ &\mathbf{E}^{(l)} = \mathbf{E}(x^{(l)}), \quad \varphi(x) = \frac{1}{\pi H}\exp\left(-\frac{|x|^2}{Hh^2}\right), \quad x^{(l)} \in V. \end{aligned} \tag{5.1}$$

Here $x^{(l)}$ is a set of nodes homogeneously distributed in the region V. After substituting approximation (5.1) into Eq. (2.1) one obtains the following equation:

$$\sum_{l=1}^{M} \mathbf{E}^{(l)}\varphi(x - x^{(l)}) + \sum_{l=1}^{M} \mathbf{I}(x - x^{(l)})c_1^{(l)} \cdot \mathbf{E}^{(l)} = \mathbf{E}(x), \quad c_1^{(m)} = c(x^{(m)}) - c_0, \tag{5.2}$$

$$I_{ij}(x) = \int K_{ij}(x - x')\varphi(x')\,\mathrm{d}x' = \frac{1}{4\pi^3 Hc_0}\int \frac{k_i k_j}{|k|^2}\exp\left(-\frac{Hh^2|k|^2}{4} - \mathrm{i}k\cdot x\right)\mathrm{d}k. \tag{5.3}$$

Eqs. (2.10) and (2.6) are used for the definition of the operator $\mathbf{K}$ in Eq. (2.1). After calculating the integrals in the right-hand side of Eq. (5.3), the tensor $\mathbf{I}(x)$ is obtained in the form:

$$I_{ij}(x) = \frac{1}{Hc_0}\left[\Phi_1(|\zeta|)\delta_{ij} + \Phi_2(|\zeta|)n_i n_j\right], \quad \zeta_i = \frac{2x_i}{h\sqrt{H}}, \quad n_i = \frac{\zeta_i}{|\zeta|}, \tag{5.4}$$

$$\Phi_1(|\zeta|) = \frac{2}{\pi|\zeta|^2}\left[1 - \exp\left(-\frac{|\zeta|^2}{4}\right)\right], \tag{5.5}$$

$$\Phi_2(|\zeta|) = \frac{4}{\pi|\zeta|^2}\left[\left(1 + \frac{|\zeta|^2}{4}\right)\exp\left(-\frac{|\zeta|^2}{4}\right) - 1\right]. \tag{5.6}$$

The system of equations for the unknowns $\mathbf{E}^{(m)} = \mathbf{E}(x^{(m)})$ follows from Eqs. (5.1) and (2.1), if the latter is to be satisfied in all the nodes $x^{(m)}$ (collocation method). As a result, the system of linear algebraic equations for the components of the vectors $\mathbf{E}^{(m)}$ is obtained in the form

$$\sum_{l=1}^{M} E_1^{(l)}\varphi(x^{(m)} - x^{(l)}) + \sum_{l=1}^{M}\left[A_{11}^{(ml)}E_1^{(l)} + A_{12}^{(ml)}E_2^{(l)}\right] = E_{01}^{(m)}, \tag{5.7}$$

$$\sum_{l=1}^{M} E_1^{(l)}\varphi(x^{(m)} - x^{(l)}) + \sum_{l=1}^{M}\left[A_{21}^{(ml)}E_1^{(l)} + A_{22}^{(ml)}E_2^{(l)}\right] = E_{02}^{(m)}. \tag{5.8}$$

Here $E_{0i}^{(l)} = E_{0i}(x^{(l)}),\ i = 1, 2$; the elements of the matrixes $A_{11},\ A_{12}$, and A_{22} are as follows:

$$A_{11}^{(ml)} = \frac{2c_1^{(l)}}{Hc_0}\left[\Phi_1\left(|\zeta^{(m)} - \zeta^{(l)}|\right) + \Phi_2\left(|\zeta^{(m)} - \zeta^{(l)}|\right)\frac{\left(\zeta_1^{(m)} - \zeta_1^{(l)}\right)^2}{|\zeta^{(m)} - \zeta^{(l)}|^2}\right], \tag{5.9}$$

$$A_{12}^{(ml)} = \frac{2c_1^{(l)}}{Hc_0}\Phi_2\left(|\zeta^{(m)} - \zeta^{(l)}|\right)\frac{\left(\zeta_1^{(m)} - \zeta_1^{(l)}\right)\left(\zeta_2^{(m)} - \zeta_2^{(l)}\right)}{|\zeta^{(m)} - \zeta^{(l)}|^2} = A_{21}^{(ml)}, \tag{5.10}$$

$$A_{22}^{(ml)} = \frac{2c_1^{(l)}}{Hc_0}\left[\Phi_1\left(|\zeta^{(m)} - \zeta^{(l)}|\right) + \Phi_2\left(|\zeta^{(m)} - \zeta^{(l)}|\right)\frac{\left(\zeta_2^{(m)} - \zeta_2^{(l)}\right)^2}{|\zeta^{(m)} - \zeta^{(l)}|^2}\right]. \tag{5.11}$$

The system (5.4) may be written in the canonical form as:

$$BX = F, \tag{5.12}$$

where the vector of unknowns X of the dimension $2M$ is defined by the equation

$$X^{(p)} = \begin{cases} E_1^{(p)}, & 1 \leqslant p \leqslant M; \\ E_2^{(p-M)}, & M < p \leqslant 2M \end{cases} \tag{5.13}$$

and vector F has the form

$$F^{(p)} = \begin{cases} E_{01}^{(p)}, & 1 \leqslant p \leqslant M; \\ E_{02}^{(p-M)}, & M < p \leqslant 2M. \end{cases} \tag{5.14}$$

The B in Eq. (5.12) is the following block-matrix of the dimension $(2M \times 2M)$

$$B = \left\| \begin{matrix} \Psi + A_{11} & A_{12} \\ A_{12} & \Psi + A_{22} \end{matrix} \right\|, \tag{5.15}$$

$$\Psi = \left\| \Psi^{(ml)} \right\|, \quad \Psi^{(ml)} = \varphi(x^{(m)} - x^{(l)}).$$

As it is seen from Eqs. (5.5), (5.6), (5.9)–(5.11), the elements of the matrix B have simple analytical forms. They are expected to be constructed much faster than the elements of the corresponding matrix when conventional approximating functions are used for the solution of the problem under consideration. Construction of the elements of B in the latter case involves numerical calculations of integrals over subareas.

The results of the calculation of the electric field in the medium with a circular inhomogeneous inclusion of a unit radius are presented in Fig. 2. The medium has dielectric permittivity $c_0 = 1$ and the dielectric properties of the inclusion changes along the radius according to a parabolic law: $c_1(r) = c(r) - c_0 = 10r^2$. The components of the constant external field applied to the medium are $E_{01} = 1, E_{02} = 0$. The bold solid lines in Fig. 2 are the exact solutions of the problem obtained by the method described in Appendix A. The thin lines are the numerical solutions constructed for a square node grid inside the circle $|x| \leqslant 1$ with the step h between the neighboring nodes. The graphs in Fig. 2(a) correspond to $H = 0.7$ and $h = 0.2$ $(M = 81)$, $h = 0.1$ $(M = 317)$, and $h = 0.05$ $(M = 1257)$. The graphs in Fig. 2(b) correspond to $H = 2$ and the same values of h. The left parts of these graphs are the dependences $E_1(0, x_2)$ on x_2 $(x_2 \geqslant 0)$, the right parts are the dependences $E_1(x_1, 0)$ on x_1 $(x_1 \geqslant 0)$. It is seen in these graphs that numerical solutions converge to the exact one with grid refinement. Again as it was pointed out in Section 4, the main error of the numerical solutions concentrates in the neighborhood of the border of the inclusion because of a non-finite support of the assumed Gaussian approximating functions.

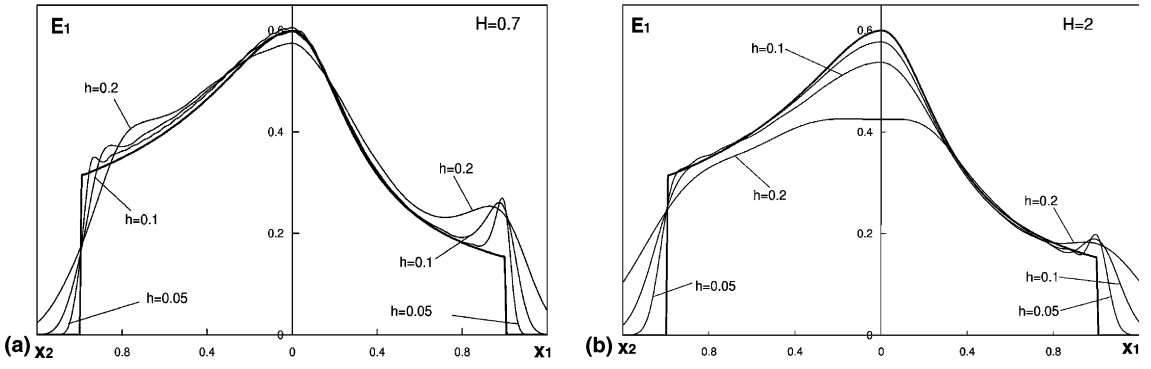

Fig. 2. Electric field $E_1(x_1, 0)$ and $E_1(0, x_2)$ inside the circular inclusion of unit radius with a parabolic distribution of dielectric permittivity along the radius $(c(r) = 1 + 10r^2)$, a constant electric field $(\mathbf{E}_0 = \mathbf{e}_1)$ is applied along x_1-axis. The thin lines are the numerical solutions using the Gaussian approximating functions, the bold lines are the exact solution.

5.2. Edge Gaussian functions

To improve the solution near the border of the region V, let us introduce 2D-Edge Gaussian functions defined similarly to functions $\widehat{\varphi}(x,a)$ in Eq. (4.7):

$$\widehat{\varphi}(x,b)=\widehat{\varphi}(x_1,x_2,b)=\begin{cases}\frac{1}{\pi H}\exp\left(-\frac{x_1^2+x_2^2}{Hh^2}\right), & x_2\leqslant b;\\ 0, & x_2>b.\end{cases} \tag{5.16}$$

If these functions are used for the approximation of the electric field $\mathbf{E}(x)$ inside region V, one has to define a local Cartesian basis $(\mathbf{e}_1^{(i)},\mathbf{e}_2^{(i)})$ at every ith node, and calculate the shortest distance $b^{(i)}$ of this node from the border Ω of the region V. Unit vector $\mathbf{e}_2^{(i)}$ of this basis has the direction of the outside normal to Ω at point $x_0^{(i)}\in\Omega$, and therefore, $x_0^{(i)}$ is the point of the border with the shortest distance $b^{(i)}$ from the node $x^{(i)}$. The global coordinates of all the nodes, the orientation of their individual local bases and the corresponding distances $b^{(i)}$ are the necessary initial data for the numerical solution in this case.

If point x has coordinates $(x-x^{(i)})_1,(x-x^{(i)})_2$ in the local basis of the ith node, the electric field $\mathbf{E}$ in this point may be approximated as follows:

$$\mathbf{E}(x)\approx\sum_{i=1}^{M}\left(\mathfrak{E}_1^{(i)}\mathbf{e}_1^{(i)}+\mathfrak{E}_2^{(i)}\mathbf{e}_2^{(i)}\right)\widehat{\varphi}\left((x-x^{(i)})_1,(x-x^{(i)})_2,b^{(i)}\right). \tag{5.17}$$

Here $\mathfrak{E}_1^{(i)},\mathfrak{E}_2^{(i)}$ are the components of the electric field in the local basis of the ith node.

The result of the action of the operator $\mathbf{K}$ on the function $\widehat{\varphi}(x_1,x_2,b)$ in Eq. (5.16) may be obtained from Eq. (2.10), taking into account that the Fourier transform of $\widehat{\varphi}(x_1,x_2,b)$ has the following form:

$$\widetilde{\widehat{\varphi}}(k_1,k_2,b)=\frac{h^2}{2}\exp(-\kappa^2)f_0(\kappa_2,\alpha),\quad f_0(\kappa,\alpha)=1+\mathrm{Erf}\left(\frac{\alpha}{2}-\mathrm{i}\kappa_2\right),\quad \kappa_i=\frac{1}{2}\sqrt{H}hk_i,$$
$$\kappa^2=\kappa_1^2+\kappa_1^2,\quad \alpha=\frac{2}{\sqrt{H}h}b,\quad \mathrm{i}=\sqrt{-1}. \tag{5.18}$$

Here $\mathrm{Erf}(z)=\frac{2}{\sqrt{\pi}}\int_0^z\exp(-t^2)\,\mathrm{d}t$ is the error-function.

After calculation of the integrals in Eq. (2.10), the following result is obtained

$$\mathbf{I}(x)=\int\mathbf{K}(x-x')\hat{\varphi}(x',b)\,\mathrm{d}x'$$
$$=\frac{1}{c_0H}[J_{11}(\zeta,\alpha)\mathbf{e}_1\otimes\mathbf{e}_1+J_{12}(\zeta,\alpha)(\mathbf{e}_1\otimes\mathbf{e}_2+\mathbf{e}_1\otimes\mathbf{e}_2)+J_{22}(\zeta,\alpha)\mathbf{e}_1\otimes\mathbf{e}_2]. \tag{5.19}$$

Here $(\mathbf{e}_1,\mathbf{e}_2)$ is the fixed Cartesian basis, $\zeta=\zeta_1\mathbf{e}_1+\zeta_2\mathbf{e}_2$, $\zeta_i=\frac{2}{h\sqrt{H}}y_i$. Functions $J_{kl}(\zeta,\alpha)$ have forms of the following integrals:

$$J_{11}(\zeta,\alpha)=\frac{1}{2\pi}\int_0^\infty\left[\frac{2}{\sqrt{\pi}}\exp\left(-\frac{\zeta_1^2}{4}-k^2\right)-F_1(k,|\zeta_1|)\right]\mathrm{Re}[f_0(k,\alpha)\exp(-\mathrm{i}k\zeta_2)]\,\mathrm{d}k, \tag{5.20}$$

$$J_{12}(\zeta,\alpha)=\frac{1}{2\pi}\int_0^\infty F_2(k,|\zeta_1|)\mathrm{Im}[f_0(k,\alpha)\exp(-\mathrm{i}k\zeta_2)]\,\mathrm{d}k, \tag{5.21}$$

$$J_{22}(\zeta,\alpha)=\frac{1}{\pi}\exp\left(-\frac{\zeta^2}{4}\right)P(\alpha-\zeta_2)-J_{11}(\zeta,\alpha), \tag{5.22}$$

where $f_0(k,\alpha)$ is defined in Eq. (5.18), functions F_1, F_2, and P in these equations are:

$$F_1(k,t) = k\Big[\mathrm{e}^{-kt}\mathrm{Erfc}\Big(k-\frac{t}{2}\Big) + \mathrm{e}^{kt}\mathrm{Erfc}\Big(k+\frac{t}{2}\Big)\Big], \tag{5.23}$$

$$F_2(k,t) = k\Big[\mathrm{e}^{-kt}\mathrm{Erfc}\Big(k-\frac{t}{2}\Big) - \mathrm{e}^{kt}\mathrm{Erfc}\Big(k+\frac{t}{2}\Big)\Big], \tag{5.24}$$

$$\mathrm{Erfc}(z) = 1 - \mathrm{Erf}(z), \tag{5.25}$$

$$P(t) = \begin{cases} 1, & t \geqslant 0; \\ 0, & t < 0. \end{cases} \tag{5.26}$$

Integrals (5.20) and (5.21) may be calculated numerically and tabulated for small values of the parameters ζ_1, ζ_2, α. For large values of $|\zeta|$ ($|\zeta| > 10$) these integrals have the following asymptotic forms:

$$J_{11}(\zeta,\alpha) \approx \frac{1}{\pi\zeta^2}\left(1 - \frac{2\zeta_1^2}{\zeta^2}\right)\Big[1 + \mathrm{Erf}\Big(\frac{\alpha}{2}\Big)\Big], \tag{5.27}$$

$$J_{12}(\zeta,\alpha) \approx -\frac{2\zeta_1\zeta_2}{\pi\zeta^4}\Big[1 + \mathrm{Erf}\Big(\frac{\alpha}{2}\Big)\Big], \tag{5.28}$$

$$J_{22}(\zeta,\alpha) \approx \frac{1}{\pi\zeta^2}\left(1 - \frac{2\zeta_2^2}{\zeta^2}\right)\Big[1 + \mathrm{Erf}\Big(\frac{\alpha}{2}\Big)\Big]. \tag{5.29}$$

Let us introduce the global Cartesian basis $(\mathbf{g}_1, \mathbf{g}_2)$. The transformation from the local basis $\mathbf{e}_1^{(i)}, \mathbf{e}_2^{(i)}$ of the ith node to its global basis may be presented in the following form:

$$\left\| \begin{matrix} \mathbf{e}_1^{(i)} \\ \mathbf{e}_2^{(i)} \end{matrix} \right\| = \left\| \begin{matrix} \cos(\beta^{(i)}) & \sin(\beta^{(i)}) \\ -\sin(\beta^{(i)}) & \cos(\beta^{(i)}) \end{matrix} \right\| \left\| \begin{matrix} \mathbf{g}_1 \\ \mathbf{g}_2 \end{matrix} \right\|, \tag{5.30}$$

where $\beta^{(i)}$ is the angle between vector $\mathbf{g}_2$ and $\mathbf{e}_2^{(i)}$.

In the global basis $\mathbf{g}_1, \mathbf{g}_2$, the electric field $\mathbf{E}(x)$ in Eq. (5.17) is presented in the form:

$$\mathbf{E}(x) \approx \sum_{i=1}^{M} \Big(E_1^{(i)}\mathbf{g}_1 + E_2^{(i)}\mathbf{g}_2\Big)\,\widehat{\varphi}\big((x-x^{(i)})_1, (x-x^{(i)})_2, b^{(i)}\big), \tag{5.31}$$

where $E_1^{(i)}, E_2^{(i)}$ are the components of the electric field in the ith node in the global basis, and $(x-x^{(i)})_1, (x-x^{(i)})_2$ are the coordinates of the vector $x - x^{(i)}$ in the ith local basis.

$$(x-x^{(i)})_1 = (x_1 - x_1^{(i)})\cos(\beta^{(i)}) + (x_2 - x_2^{(i)})\sin(\beta^{(i)}), \tag{5.32}$$

$$(x-x^{(i)})_2 = -(x_2 - x_2^{(i)})\sin(\beta^{(i)}) + (x_2 - x_2^{(i)})\cos(\beta^{(i)}). \tag{5.33}$$

Here x_1, x_2 and $x_1^{(i)}, x_2^{(i)}$ are the Cartesian coordinates of the point x and of the ith node in the global basis $\mathbf{g}_1, \mathbf{g}_2$, respectively.

The final linear algebraic system for the unknowns $E_1^{(i)}, E_2^{(i)}$ in Eq. (5.31) takes the forms (5.12)–(5.15), where elements of the matrixes $A_{11}^{(ml)}$, $A_{12}^{(ml)}$, and $A_{22}^{(ml)}$ are defined as:

$$A_{11}^{(ml)} = \frac{c_1^{(l)}}{c_0 H}\left[J_{11}^{(ml)}\cos^2(\beta^{(i)}) - J_{12}^{(ml)}\sin(2\beta^{(i)}) + J_{22}^{(ml)}\sin^2(\beta^{(i)})\right], \tag{5.34}$$

$$A_{12}^{(ml)} = \frac{c_1^{(l)}}{c_0 H}\left[J_{12}^{(ml)}\cos(2\beta^{(i)}) + \frac{1}{2}\left(J_{11}^{(ml)} - J_{22}^{(ml)}\right)\sin(2\beta^{(i)})\right], \tag{5.35}$$

$$A_{22}^{(ml)} = \frac{c_1^{(l)}}{c_0 H}\left[J_{11}^{(ml)}\sin^2(\beta^{(i)}) + J_{12}^{(ml)}\sin(2\beta^{(i)}) + J_{22}^{(ml)}\cos^2(\beta^{(i)})\right]. \tag{5.36}$$

Here $J_{rs}^{(ml)} = J_{rs}(\zeta^{(m)} - \zeta^{(l)}, \alpha^{(l)})$, functions $J_{rs}(\zeta, \alpha)$ are defined in Eqs. (5.20)–(5.29), and $\zeta^{(m)} - \zeta^{(l)}$ is dimensionless vector of the mth node in the local basis of the lth node.

The results of the numerical solutions of the problem for the inclusion with the parabolic property variation, with the help of the Edge Gaussian functions are presented in Figs. 3 and 4. Again, the bold solid lines are the exact solutions of the problem, the thin lines correspond to $h = 0.2$; 0.1; and 0.05. Fig. 3(a) corresponds to $H = 0.7$, Fig. 3(b) to $H = 2$. The results for the same calculations are presented in Fig. 4(a) for $h = 0.1$ and $H = 0.7$ and 2, and in Fig. 4(b) for $h = 0.05$ and the same values of H.

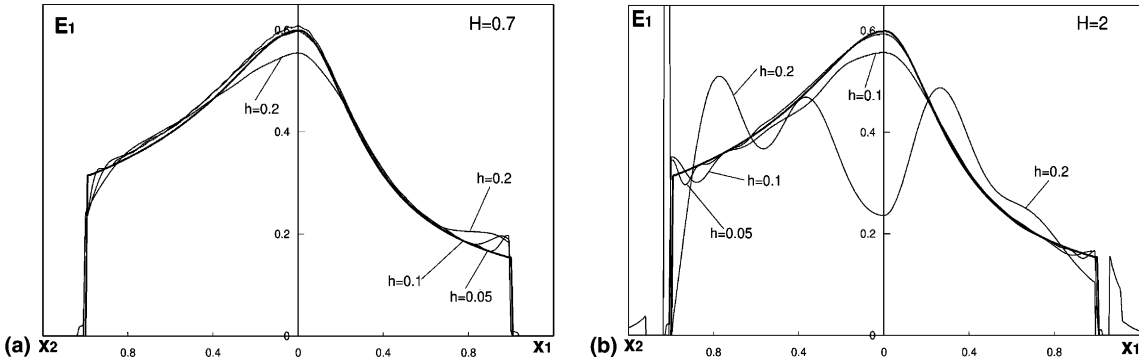

Fig. 3. The same graphs as in Fig. 2. The thin lines are the numerical solutions using the Edge Gaussian approximating functions.

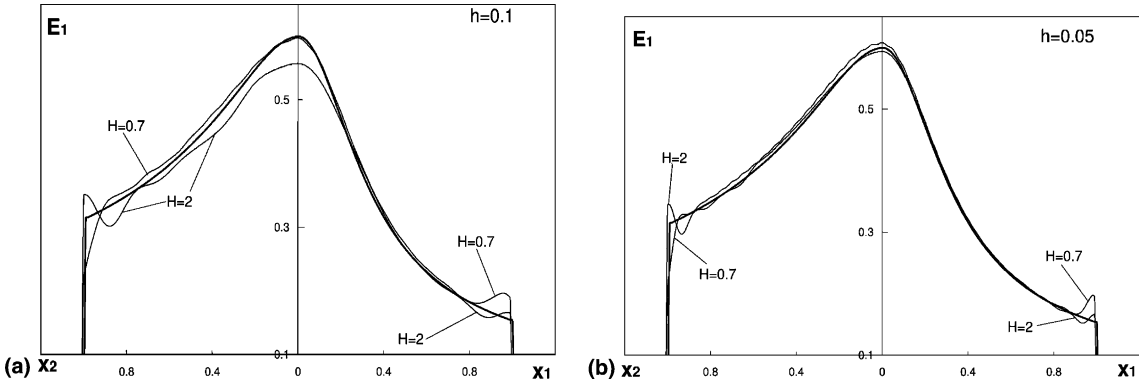

Fig. 4. The same graphs as in Fig. 3. The influence of the parameter H on the numerical solutions.

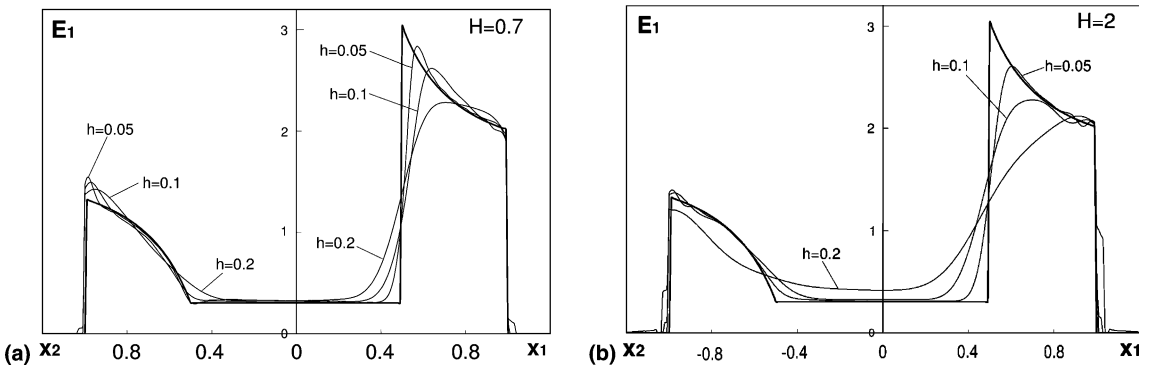

Fig. 5. Electric field $E_1(x_1,0)$ and $E_1(0,x_2)$ inside the circular layered inclusion of a unit radius, a constant electric field ($\mathbf{E}_0 = \mathbf{e}_1$) is applied along x_1-axis. Thin lines are the numerical solutions using the Gaussian approximating functions, the bold line is the exact solution.

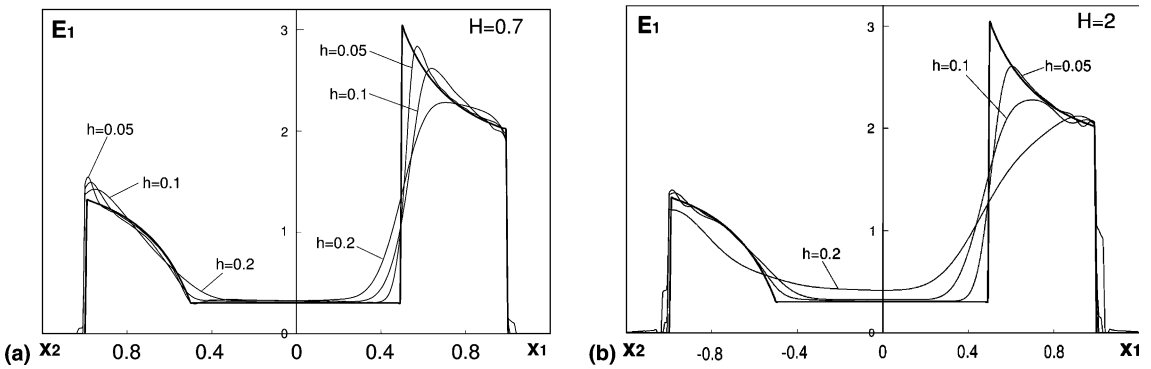

Fig. 6. The same graphs as in Fig. 5. The thin lines are the numerical solutions using the Edge Gaussian approximating functions.

The distributions of the electric field inside a layered inclusion are presented in Figs. 5 and 6. In this case, the dielectric permittivity $c(r)$ of the medium and the inclusion are defined by the equations

$$c(r) = \begin{cases} 10, & 0 \leqslant r \leqslant 0.5; \\ 1, & 0.5 < r \leqslant 1; \\ 3, & r > 1. \end{cases} \tag{5.37}$$

Jumps in the field $\mathbf{E}(x)$ are not only expected on the exterior borders of the inclusion, but also on the interior border between the layers at $r = 0.5$. The solid lines in Figs. 5 and 6 are the exact solutions of the problem, the thin lines correspond to $h = 0.2; 0.1;$ and 0.05. The graphs in Fig. 5 are the numerical solutions obtained using the Gaussian functions ($H = 0.7$ in Fig. 5(a), and $H = 2$ in Fig. 5(b)). The graphs in Fig. 6 are the numerical solutions with the Edge Gaussian approximating functions using the same parameters as above.

6. Numerical solution of Eq. (2.1) in the 3D-case

6.1. Gaussian approximating functions in the 3D-case

In the 3D-case, the basic Gaussian approximating function and its Fourier transform take the forms:

$$\varphi(x) = \frac{1}{(\pi H)^{3/2}} \exp\left(-\frac{\zeta^2}{4}\right), \quad \widetilde{\varphi}(k) = h^3 \exp\left(-\kappa^2\right), \quad \zeta_i = \frac{2}{h\sqrt{H}} x_i,$$
$$\kappa_i = \frac{h\sqrt{H}}{2} k_i, \quad \zeta^2 = \zeta_i \zeta_i, \quad \kappa^2 = \kappa_i \kappa_i. \tag{6.1}$$

The action of the operator $\mathbf{K}$ on this function is defined by the equation:

$$\mathbf{I}(x) = \int \mathbf{K}(x - x')\varphi(x')\,\mathrm{d}x' = \frac{1}{c_0 H^{3/2}} [\Psi_1(|\zeta|)\mathbf{U} + \Psi_2(|\zeta|)\mathbf{n} \otimes \mathbf{n}], \tag{6.2}$$

where $\mathbf{U}$ is the two-rank unit tensor, $n_i = \zeta_i/|\zeta|$, functions $\Psi_1(|\zeta|)$, $\Psi_2(|\zeta|)$ have the following forms:

$$\Psi_1(|\zeta|) = \frac{2}{\pi|\zeta|^3}\left[\mathrm{Erf}\left(\frac{|\zeta|}{2}\right) - \frac{|\zeta|}{\sqrt{\pi}} \exp\left(-\frac{\zeta^2}{4}\right)\right], \tag{6.3}$$

$$\Psi_2(|\zeta|) = -\frac{2}{\pi|\zeta|^3}\left[3\mathrm{Erf}\left(\frac{|\zeta|}{2}\right) - \frac{|\zeta|}{\sqrt{\pi}}\left(3 + \frac{|\zeta|}{2}\right) \exp\left(-\frac{\zeta^2}{4}\right)\right]. \tag{6.4}$$

In the fixed Cartesian basis $\mathbf{e}_1, \mathbf{e}_2, \mathbf{e}_3$ tensor $\mathbf{I}(x)$ may be also presented in the form:

$$\mathbf{I}(x) = \frac{1}{c_0 H^{3/2}} I_{ij}(\zeta)\mathbf{e}_i \otimes \mathbf{e}_j, \tag{6.5}$$

$$I_{11}(\zeta) = \Psi_1(|\zeta|) + \Psi_2(|\zeta|)\frac{\zeta_1^2}{\zeta^2}, \quad I_{22}(\zeta) = \Psi_1(|\zeta|) + \Psi_2(|\zeta|)\frac{\zeta_2^2}{\zeta^2}, \tag{6.6}$$

$$I_{33}(\zeta) = \Psi_1(|\zeta|) + \Psi_2(|\zeta|)\frac{\zeta_3^2}{\zeta^2}, \quad I_{12}(\zeta) = I_{21}(\zeta) = \Psi_2(|\zeta|)\frac{\zeta_1\zeta_2}{\zeta^2}, \tag{6.7}$$

$$I_{13}(\zeta) = I_{31}(\zeta) = \Psi_2(|\zeta|)\frac{\zeta_1\zeta_3}{\zeta^2}, \quad I_{23}(\zeta) = I_{32}(\zeta) = \Psi_2(|\zeta|)\frac{\zeta_2\zeta_3}{\zeta^2}. \tag{6.8}$$

Approximating the electric field $\mathbf{E}(x)$ inside the inclusion in the form:

$$\mathbf{E}(x) \approx \sum_{m=1}^{M} \mathbf{E}^{(m)} \varphi(x - x^{(m)}) \tag{6.9}$$

and using the collocation method will result the following linear system for the components of the vectors $\mathbf{E}^{(i)} = \mathbf{E}(x^{(m)})$ – the values of the electric field in the nodes $x^{(m)}$ $(m = 1, 2, \ldots, M)$:

$$BX = F. \tag{6.10}$$

Here the matrix-column of unknowns X of the dimension $3M$ has the form:

$$X^{(l)} = \begin{cases} E_1^{(l)}, & l \leqslant M; \\ E_2^{(l-M)}, & M < l \leqslant 2M; \\ E_3^{(l-2M)}, & 2M < l \leqslant 3M. \end{cases} \tag{6.11}$$

The right-hand side of Eq. (6.10) is defined by the components of the applied field $\mathbf{E}_0(x)$

$$F^{(l)} = \begin{cases} E_{01}^{(l)}, & l \leqslant M; \\ E_{02}^{(l-M)}, & M < l \leqslant 2M; \\ E_{03}^{(l-2M)}, & 2M < l \leqslant 3M, \end{cases} \tag{6.12}$$

where $E_{0i}^{(l)} = E_{0i}(x^{(l)})$.

Matrix B in Eq. (6.10) is the block-matrix of dimension $3M \times 3M$, composed of sub-matrices A_{rs} of dimension $M \times M$

$$B = \left\| \begin{array}{ccc} \Psi + A_{11} & A_{12} & A_{13} \\ A_{12} & \Psi + A_{22} & A_{23} \\ A_{13} & A_{23} & \Psi + A_{33} \end{array} \right\| \tag{6.13}$$

and the elements of the matrices Ψ and A_{rs} have the forms:

$$\Psi^{(ml)} = \varphi\big(x^{(m)} - x^{(l)}\big), \quad A_{rs}^{(ml)} = \frac{c_1^{(l)}}{c_0 H^{3/2}} I_{rs}\Big(\zeta^{(m)} - \zeta^{(l)}\Big). \tag{6.14}$$

Here, functions $\varphi(x)$ and $I_{rs}(\zeta)$ are defined in Eqs. (6.1) and (6.6)–(6.8).

6.2. The Edge Gaussian approximating functions in the 3D-case

In the 3D-case, the basic Edge Gaussian function is defined by the following equations:

$$\widehat{\varphi}(x,b) = \widehat{\varphi}(x_1,x_2,x_3,b) = \begin{cases} \frac{1}{(\pi H)^{3/2}} \exp\left(-\frac{x_1^2+x_2^2+x_3^2}{Hh^2}\right), & x_3 \leqslant b; \\ 0, & x_3 > b. \end{cases} \tag{6.15}$$

The Fourier transform of this function has the form:

$$\widetilde{\widehat{\varphi}}(k,b) = \frac{h^3}{2} \exp(-\kappa^2)\Big[1 + \mathrm{Erf}\Big(\frac{\alpha}{2} - \mathrm{i}\kappa_3\Big)\Big], \quad \kappa_i = \frac{h\sqrt{H}}{2} k_i, \quad \kappa^2 = \kappa_i\kappa_i, \quad \alpha = \frac{2}{h\sqrt{H}} b. \tag{6.16}$$

The action of the operator $\mathbf{K}$ on the 3D-Edge Gaussian function is presented in the form:

$$\begin{aligned} \mathbf{I}(x,b) &= \int \mathbf{K}(x-x')\widehat{\varphi}(x',b)\,\mathrm{d}x' \\ &= \frac{1}{c_0 H^{3/2}}\left[J_\theta(\zeta,\alpha)\theta + J_{ee}(\zeta,\alpha)\mathbf{e}\otimes\mathbf{e} + J_{e3}(\zeta,\alpha)(\mathbf{e}\otimes\mathbf{e}_3 + \mathbf{e}_3\otimes\mathbf{e}) + J_{33}(\zeta,\alpha)\mathbf{e}_3\otimes\mathbf{e}_3\right]. \end{aligned} \tag{6.17}$$

Here $\theta = \mathbf{e}_1\otimes\mathbf{e}_1 + \mathbf{e}_2\otimes\mathbf{e}_2$, $\mathbf{e}_1, \mathbf{e}_2, \mathbf{e}_3$ are the Cartesian basis in 3D-space,

$$\zeta_i = \frac{2}{h\sqrt{H}} x_i, \quad \mathbf{e} = \frac{1}{\sqrt{\zeta_1^2 + \zeta_2^2}}(\zeta_1\mathbf{e}_1 + \zeta_2\mathbf{e}_2). \tag{6.18}$$

Functions $J_\theta(\zeta,\alpha), J_{ee}(\zeta,\alpha)$, $J_{e3}(\zeta,\alpha)$, and $J_{33}(\zeta,\alpha)$ are the following integrals:

$$J_\theta(\zeta,\alpha) = \frac{2}{\pi\bar{\zeta}} \int_0^\infty F_1(\bar{\zeta},\kappa)\mathrm{Re}\big[\exp\big(-\mathrm{i}\zeta_3\kappa - \kappa^2\big) f_0(\kappa,\alpha)\big]\,\mathrm{d}\kappa, \tag{6.19}$$

$$J_{ee}(\zeta,\alpha) = -\frac{2}{\pi} \int_0^\infty F_2(\bar{\zeta},\kappa)\mathrm{Re}\big[\exp\big(-\mathrm{i}\zeta_3\kappa - \kappa^2\big) f_0(\kappa,\alpha)\big]\,\mathrm{d}\kappa, \tag{6.20}$$

$$J_{e3}(\zeta,\alpha)=\frac{2}{\pi}\int_0^\infty F_1(\bar{\zeta},\kappa)\kappa\mathrm{Im}\left[\exp\left(-\mathrm{i}\zeta_3\kappa-\kappa^2\right)f_0(\kappa,\alpha)\right]\mathrm{d}\kappa, \tag{6.21}$$

$$J_{33}(\zeta,\alpha)=\frac{1}{\pi}\exp\left(-\frac{\zeta^2}{4}\right)P(\alpha-\zeta_3)-\frac{2}{\pi}\int_0^\infty F_0(\bar{\zeta},\kappa)\mathrm{Im}\left[\exp\left(-\mathrm{i}\zeta_3\kappa-\kappa^2\right)f_0(\kappa,\alpha)\right]\mathrm{d}\kappa. \tag{6.22}$$

Here $\bar{\zeta}=\sqrt{\zeta_1^2+\zeta_2^2}$, functions $f_0(\kappa,\alpha)$ and $P(t)$ are defined in Eqs. (5.18) and (5.26). Functions F_0,F_1,F_2 are the following integrals:

$$F_0(\overline{\zeta},\kappa)=\frac{\kappa^2}{\pi}\int_0^\infty\frac{J_0(\overline{\zeta}t)}{\kappa^2+t^2}\exp(-t^2)\,\mathrm{d}t, \tag{6.23}$$

$$F_1(\overline{\zeta},\kappa)=\frac{1}{\pi}\int_0^\infty\frac{J_1(\overline{\zeta}t)}{\kappa^2+t^2}\exp(-t^2)t^2\,\mathrm{d}t, \tag{6.24}$$

$$F_2(\overline{\zeta},\kappa)=\frac{1}{\pi}\int_0^\infty\frac{J_2(\overline{\zeta}t)}{\kappa^2+t^2}\exp(-t^2)t^3\,\mathrm{d}t. \tag{6.25}$$

For small values of the parameter $|\zeta|$ integrals $J_\theta(\zeta,\alpha),J_{ee}(\zeta,\alpha),J_{e3}(\zeta,\alpha)$, $J_{33}(\zeta,\alpha)$ may be calculated numerically, tabulated and kept in the computer memory. For large values of $|\zeta|$ (i.e., $|\zeta|>10$) the following asymptotic formulas hold

$$J_\theta(\zeta,\alpha)\approx\frac{1}{\pi|\zeta|^3}\left[1+\mathrm{Erf}\left(\frac{\alpha}{2}\right)\right],\quad J_{ee}(\zeta,\alpha)\approx-\frac{3\overline{\zeta}^2}{\pi|\zeta|^5}\left[1+\mathrm{Erf}\left(\frac{\alpha}{2}\right)\right], \tag{6.26}$$

$$J_{e3}(\zeta,\alpha)\approx-\frac{3\overline{\zeta}\zeta_3}{\pi|\zeta|^5}\left[1+\mathrm{Erf}\left(\frac{\alpha}{2}\right)\right],\quad J_{33}(\zeta,\alpha)\approx-\frac{\overline{\zeta}^2-2\zeta_3^2}{\pi|\zeta|^5}\left[1+\mathrm{Erf}\left(\frac{\alpha}{2}\right)\right]. \tag{6.27}$$

In the Cartesian basis $\mathbf{e}_1,\mathbf{e}_2,\mathbf{e}_3$ the tensor $\mathbf{I}(x)$ in Eq. (6.17) is presented in the form:

$$\mathbf{I}(x,a)=\frac{1}{c_0H^{3/2}}\Lambda_{ij}(x,a)\mathbf{e}_i\otimes\mathbf{e}_j, \tag{6.28}$$

$$\Lambda_{11}(x,a)=J_\theta(\zeta,\alpha)+J_{ee}(\zeta,\alpha)\frac{\zeta_1^2}{\overline{\zeta}^2},\quad \Lambda_{22}(x,a)=J_\theta(\zeta,\alpha)+J_{ee}(\zeta,\alpha)\frac{\zeta_2^2}{\overline{\zeta}^2}, \tag{6.29}$$

$$\Lambda_{12}(x,a)=\Lambda_{21}(x,a)=J_{ee}(\zeta,\alpha)\frac{\zeta_1\zeta_2}{\overline{\zeta}^2},\quad \Lambda_{13}(x,a)=\Lambda_{31}(x,a)=J_{e3}(\zeta,\alpha)\frac{\zeta_1}{\overline{\zeta}}, \tag{6.30}$$

$$\Lambda_{23}(x,a)=\Lambda_{32}(x,a)=J_{e3}(\zeta,\alpha)\frac{\zeta_2}{\overline{\zeta}},\quad \Lambda_{33}(x,a)=J_{33}(\zeta,\alpha). \tag{6.31}$$

For the use of the Edge Gaussian functions, the shortest distance $b^{(i)}$ from the ith node and the border Ω of the region V as well as the orientation of the local basis at the ith node should be defined. The direction of the vector $\mathbf{e}_3^{(i)}$ of the local basis should coincide with the normal $\mathbf{n}^{(i)}$ to the surface Ω at point $x_0^{(i)}\in\Omega$ that is on the line along the shortest distance from the ith node to that border.

Let us introduce a global Cartesian basis $(\mathbf{g}_1, \mathbf{g}_2, \mathbf{g}_3)$ and a global spherical coordinate system (θ, φ, r) with the same origins. The polar axis of the spherical system is directed along vector $\mathbf{g}_3$, and φ is the angle between the vector $\mathbf{g}_1$ and the projection of the vector x on the plane $(\mathbf{g}_1, \mathbf{g}_2)$. Let us move the vector $\mathbf{n}^{(i)}$ normal to the surface Ω at point $x_0^{(i)}$, into the origin of the global spherical coordinate system using parallel transfer, and let the spherical coordinates of the moved vector be $(\theta^{(i)}, \varphi^{(i)}, 1)$. Local Cartesian basis $(\mathbf{e}_1^{(i)}, \mathbf{e}_2^{(i)}, \mathbf{e}_3^{(i)})$ at the ith node is constructed by parallel transferring the basis $(\mathbf{e}_\theta, \mathbf{e}_\varphi, \mathbf{e}_r)$ of the global spherical system at point $(\theta^{(i)}, \varphi^{(i)}, 1)$ to the ith node $x^{(i)}$:

$$\mathbf{e}_1^{(i)} = \mathbf{e}_\theta(\theta^{(i)}, \varphi^{(i)}, 1), \quad \mathbf{e}_2^{(i)} = \mathbf{e}_\varphi(\theta^{(i)}, \varphi^{(i)}, 1), \quad \mathbf{e}_3^{(i)} = \mathbf{e}_r(\theta^{(i)}, \varphi^{(i)}, 1) = \mathbf{n}^{(i)}. \tag{6.32}$$

The basis vectors of the local and global Cartesian systems are related by the equations

$$\mathbf{e}_l^{(i)} = \sum_{k=1}^{3} Q_{lk}^{(i)} \mathbf{g}_k, \quad \mathbf{g}_l = \sum_{k=1}^{3} \overline{Q}_{lk}^{(i)} \mathbf{e}_k^{(i)}, \tag{6.33}$$

where $Q_{lk}^{(i)}$ and $\overline{Q}_{lk}^{(i)}$ are the components of the matrix $\mathbf{Q}^{(i)}$ and of the matrix $\overline{\mathbf{Q}}^{(i)}$ transposed with respect to $\mathbf{Q}^{(i)}$. The matrix $\mathbf{Q}^{(i)}$ has the form

$$\mathbf{Q}^{(i)} = \left\| \begin{array}{ccc} \cos\theta^{(i)} \cos\varphi^{(i)} & \cos\theta^{(i)} \sin\varphi^{(i)} & -\sin\theta^{(i)} \\ -\sin\varphi^{(i)} & \cos\varphi^{(i)} & 0 \\ \sin\theta^{(i)} \cos\varphi^{(i)} & \sin\theta^{(i)} \sin\varphi^{(i)} & \cos\theta^{(i)} \end{array} \right\|. \tag{6.34}$$

The electric field in the inclusion is approximated by the equation:

$$\mathbf{E}(x) \approx \sum_{i=1}^{M} \mathbf{E}^{(i)} \hat{\varphi}\left((x - x^{(i)})_1, (x - x^{(i)})_2, (x - x^{(i)})_3, b^{(i)}\right). \tag{6.35}$$

Here $(x - x^{(i)})_j$ $(j = 1, 2, 3)$ are the coordinates of vector $x - x^{(i)}$ in the local basis of the ith node.

After application of the collocation method to the solution of the original integral equation the linear system for the components of the vectors $\mathbf{E}^{(i)} = \mathbf{E}(x^{(i)})$ in the global basis $\mathbf{g}_1, \mathbf{g}_2, \mathbf{g}_3$ will take the following form:

$$\sum_{j=1}^{M} E_1^{(j)} \boldsymbol{\Psi}^{(ij)} + \sum_{j=1}^{M} \frac{c_1^{(j)}}{c_0 H^{3/2}} \left[\widehat{\boldsymbol{\Lambda}}_{11}^{(ij)} E_1^{(j)} + \widehat{\boldsymbol{\Lambda}}_{12}^{(ij)} E_2^{(j)} + \widehat{\boldsymbol{\Lambda}}_{13}^{(ij)} E_3^{(j)} \right] = E_{01}^{(i)}, \tag{6.36}$$

$$\sum_{j=1}^{M} E_2^{(i)} \boldsymbol{\Psi}^{(ij)} + \sum_{j=1}^{M} \frac{c_1^{(j)}}{c_0 H^{3/2}} \left[\widehat{\boldsymbol{\Lambda}}_{12}^{(ij)} E_1^{(j)} + \widehat{\boldsymbol{\Lambda}}_{22}^{(ij)} E_2^{(j)} + \widehat{\boldsymbol{\Lambda}}_{23}^{(ij)} E_3^{(j)} \right] = E_{02}^{(i)}, \tag{6.37}$$

$$\sum_{j=1}^{M} E_3^{(i)} \boldsymbol{\Psi}^{(ij)} + \sum_{j=1}^{M} \frac{c_1^{(j)}}{c_0 H^{3/2}} \left[\widehat{\boldsymbol{\Lambda}}_{13}^{(ij)} E_1^{(j)} + \widehat{\boldsymbol{\Lambda}}_{23}^{(ij)} E_2^{(j)} + \widehat{\boldsymbol{\Lambda}}_{33}^{(ij)} E_3^{(j)} \right] = E_{03}^{(i)}. \tag{6.38}$$

Here,

$$\widehat{\boldsymbol{\Lambda}}_{mn}^{(ij)} = \sum_{k,l=1}^{3} Q_{mk}^{(j)} Q_{nl}^{(j)} \Lambda_{kl}\left(\zeta^{(i)} - \zeta^{(j)}, \alpha^{(j)}\right), \quad m, n = 1, 2, 3 \tag{6.39}$$

and functions $\Lambda_{kl}(\zeta, \alpha)$ are defined in Eqs. (6.29)–(6.31).

The linear system defined by Eqs. (6.36)–(6.38) may be rewritten in the canonical form:

$$BX = F, \tag{6.40}$$

where the block-square matrix B of the dimension $(3M \times 3M)$ has the form

$$B = \left\| \begin{array}{ccc} \Psi + A_{11} & A_{12} & A_{13} \\ A_{12} & \Psi + A_{22} & A_{23} \\ A_{13} & A_{23} & \Psi + A_{33} \end{array} \right\|, \tag{6.41}$$

$$A_{mn} = \frac{c_1^{(j)}}{c_0 H^{3/2}} \widehat{A}_{mn}^{(ij)}, \quad i,j \leqslant M, \quad m,n = 1,2,3 \tag{6.42}$$

and the components of the matrix Ψ are defined in Eq. (6.14). The components of vectors X and F are:

$$X^{(i)} = \begin{cases} E_1^{(i)}, & i \leqslant M; \\ E_2^{(i-M)}, & M < i \leqslant 2M; \\ E_2^{(i-2M)}, & 2M < i \leqslant 3M; \end{cases} \tag{6.43}$$

$$F^{(i)} = \begin{cases} E_{01}(x^{(i)}), & i \leqslant M; \\ E_{02}(x^{(i-M)}), & M < i \leqslant 2M; \\ E_{02}^{(i-2M)}, & 2M < i \leqslant 3M. \end{cases} \tag{6.44}$$

The results of the calculation of the electric field inside a spherical inclusion with the parabolic distribution of the properties ($c(r) = 1 + 10r^2$, $r \leqslant 1$; $c(r) = 1$, $r > 1$) are presented in Figs. 7(a) and (b). The external field is constant and has components $E_1 = 1$, $E_2 = E_3 = 0$. The dependences $E_1(x_1, 0, 0)$ for $x_1 \geqslant 0$ are on the right-hand sides of these figures, and the dependences $E_1(0, x_2, 0)$ for $x_2 \geqslant 0$ are on their left-hand sides. All calculations were carried out using a cubic grid with step h. The results of the calculations for values $H = 0.7$; 1.5; and $h = 0.1$; 0.2 are presented in these figures by thin solid lines, the bold lines are exact distributions of the electric field obtained by the method described in Appendix A.

The distribution of the electric field inside a spherical layered inclusion ($c(r) = 10$, $0 \leqslant r \leqslant 0.5$; $c(r) = 1$, $0.5 < r \leqslant 1$; $c(r) = 3$, $r > 1$) is presented in Figs. 8(a) and (b). The external field has components $E_1 = 1$, $E_2 = E_3 = 0$ in the global basis. The dependences $E_1(x_1, 0, 0)$ for $x_1 \geqslant 0$ are on the right-hand sides of these figures, and $E_1(0, x_2, 0)$ for $x_2 \geqslant 0$ are on their left-hand sides. The results of the calculations for $H = 0.7$; 1;

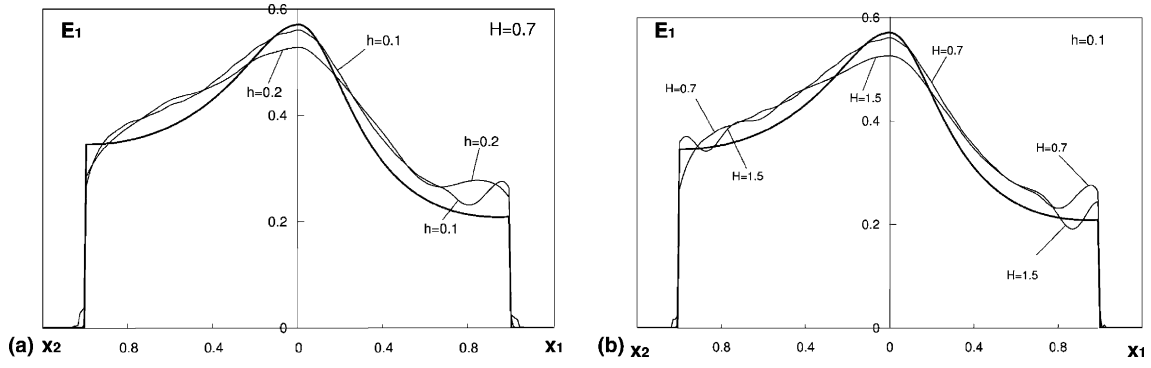

Fig. 7. Electric field $E_1(x_1, 0, 0)$ and $E_1(0, x_2, 0)$ inside the spherical inclusion of a unit radius with the parabolic distribution of dielectric permittivity along the radius ($c(r) = 1 + 10r^2$), a constant electric field ($\mathbf{E}_0 = \mathbf{e}_1$) is applied along x_1-axis. The thin lines are the numerical solutions using the Edge Gaussian approximating functions, the bold lines are the exact solutions.

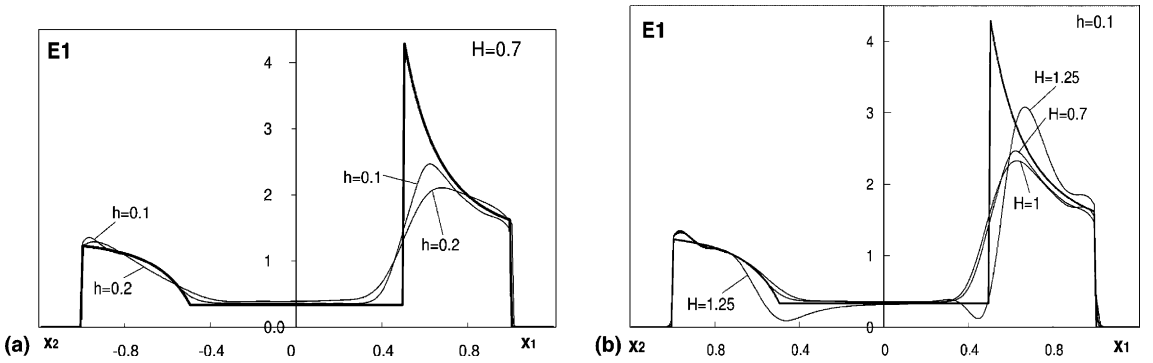

Fig. 8. Electric field $E_1(x_1,0,0)$ and $E_1(0,x_2,0)$ inside the spherical layered inclusion of a unit radius, a constant electric field ($\mathbf{E}_0 = \mathbf{e}_1$) is applied along x_1-axis. Thin lines are numerical solutions using the Edge Gaussian approximating functions, the bold lines are the exact solutions.

1.25 and $h = 0.1$; 0.2 are presented in these figures by thin solid lines, the bold lines are the exact distribution of the electric field.

7. Conclusion

The Gaussian approximating functions are an efficient tool for the solution of the volume integral equations of the thermo- and electro-static problems for the medium with inhomogeneous inclusions. The use of these functions has the advantage of fast construction of the matrix of the linear algebraic system obtained after the discretization of the problem. If the Edge Gaussian functions are used, it is assumed that the basic functions $J_{11}(\zeta,\alpha)$, $J_{12}(\zeta,\alpha)$ in Eqs. (5.20)–(5.22) for the 2D-case or functions $J_\theta(\zeta,b)$, $J_{ee}(\zeta,\alpha)$, $J_{e3}(\zeta,\alpha)$ and $J_{33}(\zeta,\alpha)$ for the 3D-case are previously tabulated and kept in the computer memory.

However, the numerical accuracy strongly depends on the step h of the node grid used in the calculations as well as on the type of the approximating functions. The accuracy near the border of the inclusion essentially increases if the Edge Gaussian functions are used (comparing Figs. 3 and 4, and Figs. 6 and 7). For the parabolic distribution of properties inside a circular inclusion of a unit radius, the numerical solutions at a grid resolution $h = 0.05$ and based on the Edge Gaussian functions practically coincides with the corresponding exact solutions (see Figs. 4 and 6). The influence of parameter H in the approximations (5.1) and (5.17) on the accuracy of the numerical solution is more pronounced at relatively large h ($h > 0.1$). At small h ($h < 0.05$) and $0.5 < H < 2$ the numerical solution is not sensitive to H. On the other hand, outside this range of H, the convergence of the method with respect to h is worse.

If the properties inside the inclusion have a step change (jump), the fields near this jump should be calculated with sufficient accuracy and, as demonstrated in Fig. 6, relatively small values of the parameter h have to be chosen. On the other hand, if some integral characteristics of the fields are the aim of the calculations (e.g., the mean values of fields over the inclusion), the overall accuracy of the solution will be less sensitive to the resolution h, resulting in smaller number of equations and faster calculation times.

The general behavior in the 3D-case is similar to the 2D-case. Signifying achievement of the same accuracy as in the 2D-case (i.e., $h = 0.05$), will require multiple fold increase in the number of necessary grid nodes. For instance, for the spherical inclusion of a unit radius and $h = 0.05$, the number of nodes is $M = 32{,}960$, and the matrix B of the discretized system has $(3M \times 3M)$ elements. It should be noted that B is a dense matrix with maximal terms near the main diagonal. It consists of six sub-matrices of dimensions $(M \times M)$ in a block matrix fashion. Although it marginally allows reduction of the volume of the memory that is necessary to keep matrix B, nevertheless, for the solution 3D-problems, one has to use powerful

computers with sufficient accessible storage memory. For the problems considered in this study the conditional number of the matrix B turned to be about 10, and LU-decomposition algorithm was extensively used for the solution of the final linear algebraic systems of the discretized problems.

Note that all calculations carried out in this study were only based on homogeneous grids of nodes. But non-homogeneous grids may be also used in the framework of the method. The theoretical background of the approximation by the Gaussian functions and non-homogeneous node grids was developed in [14].

The method developed in this work for the solution of the thermo- and electro-static problems of composite media may be applied to a wide class of the problems of mathematical physics that are reduced to volume or superficial integral equations. In particular, the problems of elasticity and elasto-plasticity, the problems of elastic and electro magnetic wave diffraction on inclusions may be successfully solved with the help of this class of the approximation functions.

Acknowledgements

This work was supported by CONACYT(Mexico) and Texas A&M University joined research program.

Appendix A

The equation for the tensor $\mathbf{A}(x)$ in the presentation (3.1) of the solution in the case spherically symmetric inclusion follows from Eq. (2.1) in the form:

$$\mathbf{A}(x) + (\mathbf{K} \cdot c_1\mathbf{A})(x) = -(\mathbf{K}c_1)(x). \tag{A.1}$$

The action of the operator $\mathbf{K}$ on a piecewise smooth function f with a compact support may be presented in the following form [13]:

$$(\mathbf{K}f)(r,\mathbf{n}) = \frac{1}{2\pi\mathrm{i}} \int_{\tau-\mathrm{i}\infty}^{\tau+\mathrm{i}\infty} r^{-s}(\mathbf{K}_s f^*)(s,\mathbf{n})\,\mathrm{d}s. \tag{A.2}$$

Here $r = |x|, \mathbf{n} = x/r$, $f^*(s,n)$ is the Mellin transform of function $f(r,n)$ in respect with argument r,

$$f^*(s,\mathbf{n}) = \int_0^\infty f(r,\mathbf{n}) r^{s-1}\,\mathrm{d}r, \quad f(r,\mathbf{n}) = \frac{1}{2\pi\mathrm{i}} \int_{\tau-\mathrm{i}\infty}^{\tau+\mathrm{i}\infty} r^{-s} f^*(s,\mathbf{n})\,\mathrm{d}s. \tag{A.3}$$

Operator $\mathbf{K}_s$ in Eq. (A.3) is defined by the following equation [13]:

$$(\mathbf{K}_s f^*)(s,\mathbf{n}) = \frac{\exp(\mathrm{i}(\pi d/2))}{(2\pi)^d} \Gamma(d-s)\Gamma(s) \int_{\Omega_1} (-\mathbf{n}\cdot\mathbf{m})^{-s}\,\mathrm{d}\mathbf{m} \int_{\Omega_1} \widetilde{\mathbf{K}}(\mathbf{m}) f^*(s,\mathbf{l})(\mathbf{m}\cdot\mathbf{l})^{s-d}\,\mathrm{d}\mathbf{m}. \tag{A.4}$$

Here d is the dimension of space, $\Gamma(s)$ is Euler's gamma function, Ω_1 is the surface of a unit sphere in d-space, $\mathbf{n}, \mathbf{m}, \mathbf{l}$ are vectors on Ω_1. Tensor $\widetilde{\mathbf{K}}(\mathbf{m})$ in this equation is defined in Eq. (2.6).

After applying the Mellin transform with respect to variable r to both sides of Eq. (A.1) we go to the following equation

$$\mathbf{A}^*(s,\mathbf{n}) + (\mathbf{K}_s \cdot (c_1\mathbf{A})^*)(s,\mathbf{n}) = -(\mathbf{K}_s c_1^*)(s,\mathbf{n}). \tag{A.5}$$

Direct calculations using Eq. (A.4) show that the right-hand side of this equation has the form:

$$(\mathbf{K}_s c_1^*)(s,\mathbf{n}) = \frac{c_1^*(s)}{c_0}\mathbf{T}(s,\mathbf{n}), \quad \mathbf{T}(s,\mathbf{n}) = \frac{1}{d-s}(\mathbf{U} - s\mathbf{n}\otimes\mathbf{n}), \tag{A.6}$$

where $\mathbf{U}$ is the unit two rank tensor.

It turns out that Eq. (A.5) may be satisfied by the following tensor:

$$\mathbf{A}^*(s,\mathbf{n}) = \alpha^*(s)(d-s)\mathbf{T}(s,\mathbf{n}). \tag{A.7}$$

After substituting Eq. (A.7) into Eq. (A.5) and taking into account that

$$(\mathbf{K}_s \cdot \mathbf{T})(s,\mathbf{n}) = \frac{1}{c_0}\mathbf{T}(s,\mathbf{n}) \tag{A.8}$$

we obtain an equation which both sides are proportional to the tensor $\mathbf{T}(s,\mathbf{n})$. From the equivalence of the coefficients in front of this tensor in the right- and left-hand sides of this equation follows the equation for the Mellin transform of the function $\alpha^*(s)$:

$$s(d-s)\alpha^*(s) + \frac{s}{c_0}s(c_1\alpha)^*(s) + \frac{(s-d+1)}{c_0}(c_1 D\alpha)^*(s) = -\frac{c_1^*(s)}{c_0}, \quad D = r\frac{\mathrm{d}}{\mathrm{d}r}. \tag{A.9}$$

Applying to this equation the inverse Mellin transform and taking into account that multiplier s corresponds to the operator D in the r-space we obtain the ordinary differential equation for the function $\alpha(r)$. Function $\alpha(r)$ should satisfy the following conditions in the origin and at infinity:

$$\alpha(0) < \infty, \quad \alpha(r) \to 0 \quad \text{if } r \to \infty. \tag{A.10}$$

If function $\alpha(r)$ is constructed, tensor $\mathbf{A}(r,n)$ takes the form:

$$\mathbf{A}(r,\mathbf{n}) = (\mathbf{U} + \mathbf{n}\otimes\mathbf{n}D)\alpha(r) \tag{A.11}$$

that follows from Eqs. (A.6) and (A.7).

The differential equation for $\alpha(r)$ is dramatically simplified in the case of spherically layered inclusions. In this case $c_1(r)$ is a step-wise constant function

$$c_1(r) = c_1^{(i)} = \text{const}, \quad a^{(i-1)} < r < a^{(i)}, \tag{A.12}$$

and the differential equation for $\alpha(r)$ inside every layer takes the form:

$$D(d+D)\alpha = 0, \quad a^{(i-1)} < r < a^{(i)}. \tag{A.13}$$

The general solution of this equation is:

$$\alpha(r) = Y_1^{(i)} + Y_2^{(i)} r^{-d}. \tag{A.14}$$

Additional analysis shows that on the borders of the layers the following conditions hold

$$[\alpha]_i = 0, \quad [cD\alpha]_i = -\big(1 + \alpha(a^{(i)})\big)[c]_i. \tag{A.15}$$

Here $[f]_i = f(a^{(i)}+0) - f(a^{(i)}-0)$, $\quad f(a^{(i)} \pm 0) = \lim_{\varepsilon\to 0} f(a^{(i)} \pm \varepsilon)$, $\quad \varepsilon > 0$.

The mentioned properties of the solution in the case of layered inclusion allow to propose the following algorithm of the construction of all the constants $Y_1^{(i)}, Y_2^{(i)}$ $(i = 1,2,\ldots,N)$ in Eq. (A.14). Let us introduce two vectors inside every ith layer:

$$X^{(i)}(r) = \left\| \begin{matrix} X_1^{(i)}(r) \\ X_2^{(i)}(r) \end{matrix} \right\|, \quad Y^{(i)} = \left\| \begin{matrix} Y_1^{(i)} \\ Y_2^{(i)} \end{matrix} \right\|, \tag{A.16}$$

$$X_1^{(i)}(r) = \alpha(r), \quad X_1^{(i)}(r) = D\alpha(r), \quad a^{(i-1)} < r < a^{(i)}.$$

The connection between these two vectors has the form that follows from Eq. (A.14)

$$X^{(i)}(r) = T(r)Y^{(i)}, \quad a^{(i-1)} < r < a^{(i)}; \tag{A.17}$$

$$T(r) = \left\| \begin{matrix} 1 & r^{-d} \\ 0 & -\mathrm{d}r^{-d} \end{matrix} \right\|.$$

Thus, one can defined the operation of the transition of the solution $X^{(i)}$ through the ith layer

$$X^{(i)}(a^{(i)}) = R^{(i)}X^{(i)}(a^{(i-1)}), \quad R^{(i)} = T(a^{(i)})T(a^{(i-1)}). \tag{A.18}$$

The law of transition of the solution through the border $r = a^{(i)}$ between two layers follows from Eq. (A.15) in the form

$$X^{(i+1)}(a^{(i)}) = F^{(i)} + \Gamma^{(i)}X^{(i)}(a^{(i)}), \tag{A.19}$$

$$F^{(i)} = \left\| \begin{matrix} 0 \\ \frac{c^{(i)}-c^{(i+1)}}{c^{(i+1)}} \end{matrix} \right\|, \quad \Gamma^{(i)} = \left\| \begin{matrix} 1 & 0 \\ \frac{c^{(i)}-c^{(i+1)}}{c^{(i+1)}} & \frac{c^{(i)}}{c^{(i+1)}} \end{matrix} \right\|. \tag{A.20}$$

These equations allow us to define the solution in the ith layer via the solution in the first layer

$$X^{(i+1)}(a^{(i)}) = g^{(i)} + G^{(i)}X^{(1)}(a^{(1)}), \tag{A.21}$$

$$g^{(i)} = F^{(i)} + \sum_{j=1}^{i-1} G_g(i,j)F^{(j)}, \quad G_g(i,j) = Q^{(i)}Q^{(i-1)} \cdots Q^{(i-j+1)}, \tag{A.22}$$

$$Q^{(i)} = \Gamma^{(i)}R^{(i)}, \quad G^{(i)} = Q^{(i)}Q^{(i-1)} \cdots Q^{(1)}, \quad R^{(1)} = U = \left\|\delta_{ij}\right\|.$$

Now, from the boundary conditions (A.10) we obtain

$$X_1^{(1)} = Y_1^{(1)}, \quad X_2^{(1)} = 0; \quad Y_2^{(1)} = 0;$$

$$X_1^{(N+1)} = Y_2^{(N+1)}r^{-d}, \quad X_2^{(N+1)} = -dY_2^{(N+1)}r^{-d}, \quad Y_1^{(N+1)} = 0. \tag{A.23}$$

From Eqs. (A.23) and (A.21) we have

$$g_1^{(N)} + G_{11}^{(N)}Y_1^{(1)} = Y_2^{(N+1)}(a^{(N)})^{-d}, \quad g_2^{(N)} + G_{21}^{(N)}Y_1^{(1)} = -dY_2^{(N+1)}(a^{(N)})^{-d}. \tag{A.24}$$

Excluding $Y_2^{(N+1)}$ from these two equations we obtain the constant $Y_1^{(1)}$ in the form

$$Y_1^{(1)} = -\frac{dg_1^{(N)} + g_2^{(N)}}{dG_{11}^{(N)} + G_{21}^{(N)}}. \tag{A.25}$$

After calculation of $Y_1^{(1)}$ one can fined all the vectors $Y^{(i)}$ from the equations

$$Y^{(i+1)} = T^{-1}(a^{(i)})X^{(i+1)}(a^{(i)}), \quad X^{(i+1)}(a^{(i)}) = g^{(i)} + G^{(i)}Y^{(1)}, \quad Y^{(1)} = \{Y_1^{(1)}, 0\} \tag{A.26}$$

that follow from Eqs. (A.17). Thus, the problem is converted to the multiplications of the matrixes and vectors of the order (2×2) and 2.

Using these algorithms the solutions of the problem for the inclusion with a continuous property changing along the radius may be obtained by step wise constant approximation of the original function

$c(r)$. For the solution of the problem with parabolic distribution of the properties along the radius of the inclusion considered in Section 5 and 6, the following parameters of the layers were chosen $a^{(i)} = \frac{i}{N}$, $i = 1, 2, \ldots, N$; $c_1(r) = 10(a^{(i)})^2$, $a^{(i-1)} < r < a^{(i)}$. If $N > 100$ the solution does not change practically when N increases. In the calculations in Sections 5 and 6, $N = 1000$ was taken.

References

[1] W.Ch. Chew, Waves and Fields in Inhomogeneous Media, Van Nostrand Reinhold, 1990.
[2] A.F. Peterson, S.L. Ray, R. Mittra, Computational Methods for Electromagnetics, IEEE Press, NY, 1997.
[3] V. Maz'ya, A new approximation method and its applications to the calculation of volume potentials. Boundary point method, in: 3. DFG-Koloqium des DFG-Forschungs schwerpunctes 'Randelementmethoden', 1991.
[4] V. Maz'ya, Approximate approximation, in: J.R. Whitman (Ed.), The Mathematics of Finite Elements and Applications. Highlights 1993, vol. 77, Wiley, Chichester, 1994.
[5] V. Maz'ya, G. Shmidt, On approximate approximations using Gaussian kernels, IMA J. Numer. Anal. 16 (1996) 13.
[6] V. Maz'ya, G. Shmidt, Approximate wavelets and the approximation of pseudodifferential operators, Appl. Comput. Harm. Anal. 6 (1999) 287.
[7] S.K. Kanaun, V. Romero, J. Bernal, A new numerical method for the solution of the second boundary value problem of elasticity for bodies with cracks, Revista Mexicana de Física 47 (2001) 309.
[8] S.K. Kanaun, V. Romero, Boundary point method in the dynamic problems of elasticity for plane areas with cracks, Int. J. Fract. 111 (2001) L3.
[9] S.K. Kanaun, A method for the solution of the diffraction problem on perfectly conducting screens, J. Comput. Phys. 176 (Feb) (2002) 170.
[10] S.G. Mikhlin, Many Dimension Singular Integrals and Integral Equations, (in Russian) FM, Moscow, 1962.
[11] I.A. Kunin, The Theory of Elastic Media with Microstructure, vol. 2, Springer Verlag, Berlin, New York, Toronto, 1983.
[12] S.K. Kanaun, L.T. Kudrjavtseva, Spherically layered inclusions in a homogeneous elastic medium, Appl. Math. Mech. (PMM) 50 (1986) 633.
[13] B.A. Plamenevsky, About the boundedness of singular operators in the weight spaces, Math. Collect. (Mat. Sbornik) 76 (1968) 573.
[14] A.G. Maz'ya, G. Schmidt, On quasi-interpolation with non-uniformly distributed centers on domains and manifolds, J. Approx. Theory 110 (2001) 125.